Spontaneous creation of discrete breathers in Josephson arrays

M. Schuster, F. Pignatelli, and A. V. Ustinov
Physikalisches Institut III, Universität Erlangen-Nürnberg, Erwin-Rommel-Straße 1, 91058 Erlangen, Germany
(Received 12 September 2003; revised manuscript received 15 December 2003; published 11 March 2004)

We report on the experimental generation of discrete breather states (intrinsic localized modes) in frustrated Josephson arrays. Our experiments indicate the formation of discrete breathers during the transition from the static to the dynamic (whirling) system state, induced by a uniform external current. Moreover, spatially extended resonant states, driven by a uniform current, are observed to evolve into localized breather states. Experiments were performed on single Josephson plaquettes as well as open-ended Josephson ladders with 10 and 20 cells. We interpret the breather formation as the result of the penetration of vortices into the system.

DOI: 10.1103/PhysRevB.69.094507 PACS number(s): 74.50.+r, 63.20.Pw, 05.45.Yv

Discrete breathers (DB's) are spatially localized, time-periodic excitations of spatially uniform nonlinear lattices. After initial theoretical studies,[1,2] they were observed in experiments in a variety of systems.[3–6] In arrays of superconducting Josephson junctions, so-called Josephson ladders (JL's), DB's can be excited in a controlled way.[5–7] Experiments that were carried out in JL's ranging from one cell up to several tens of cells revealed a large variety of possible DB states.[8] The region of existence and the resonant interaction of the nonlinear DB excitation with linear waves were studied.[9,10]

DB states in JL are usually excited from the uniform static state of the lattice by using additional currents (i.e., local forces) which are removed after the DB creation. This well-controlled procedure helps one to study DB properties systematically. In this paper we report that DB can be also excited without applying any local forces to the lattice. We present several scenarios where DB states are observed to form spontaneously. The DB formation may occur either from the initially static system state, or as a ''breakdown'' of spatially extended whirling states that are in resonance with the cavity eigenfrequency.

Within the RCSJ (resistively and capacitively shunted junction) model,[11] a Josephson junction (JJ) has a simple mechanical analog, which is a pendulum. In this analog, the difference φ of the superconducting phases across the JJ corresponds to the pendulum tilting angle. The current sent across the JJ is represented by a torque γ applied to the pendulum. Both JJ and pendulum are subject to a velocity dependent friction force $\alpha\dot{\varphi}$ with damping constant α. In the case considered here, the damping is small, $\alpha \ll 1$. The JJ or pendulum phase moves in a cosine potential due to the Josephson energy or gravitation, respectively, which leads to a force proportional to $\sin\varphi$. The dynamical equation governing the phase motion can in either case be written in normalized units as

$$\ddot{\varphi} + \alpha\dot{\varphi} + \sin\varphi = \gamma. \tag{1}$$

The time-averaged solutions $\langle\varphi\rangle$ and $\langle\dot{\varphi}\rangle$ of this equation have several simple forms,[11] depending on the value of γ. Equation (1) is symmetric for $\gamma \to -\gamma$, $\varphi \to -\varphi$, hence we restrict the following consideration to $\gamma \geqslant 0$. For $4\alpha/\pi < \gamma < \infty$, a *whirling* solution exists (corresponding to a stable limit cycle in phase space), with $\langle\dot{\varphi}\rangle = \gamma/\alpha \Leftrightarrow \langle\varphi\rangle = (\gamma/\alpha)t$. For $0 < \gamma < 1$, there also exists a *static* solution (a fixed point in phase space) with $\langle\varphi\rangle = \arcsin\gamma$. For the intermediate range $4\alpha/\pi \leqslant \gamma \leqslant 1$, both solutions are possible. Which of the solutions the system tends to depends on the initial conditions, hence the pendulum is hysteretic. Due to the Josephson law, the time derivative of the phase is proportional to the voltage drop across the JJ. For the whirling solution, the normalized voltage v is therefore proportional to the current γ, $v = \langle\dot{\varphi}\rangle = (1/\alpha)\gamma$, and the inverse of the damping α is simply the (normalized) ohmic resistance r of the JJ, $r = 1/\alpha$. The real current I is normalized to the maximum current allowing for the static state I_c, hence $\gamma = I/I_c$, for convenience.

A JL is a single row of a two-dimensional rectangular Josephson junction array [see Fig. 1(b)]. The JJ's are connected via superconducting leads. JJ's on the spars of the ladder will be referred to as the ''vertical'' junctions, those along the rungs as ''horizontal'' junctions. The vertical JJ's are all identical and have an area of A_v, likewise all horizontal JJ's are identical but have an area A_h. The elementary cell of the ladder consists of two vertical and two horizontal JJ's. Many of the properties from the extended Josephson ladder are preserved in a single cell with only one horizontal JJ [Fig. 1(a)]. This system is the simplest possible Josephson array permitting DB-like excitations. The anisotropy η is defined as the ratio of the horizontal and vertical JJ areas, $\eta = A_h/A_v$. The JJ phases inside a cell are coupled due to the magnetic flux quantization and via a circulating inductive current. Every cell has a self-inductance L. A

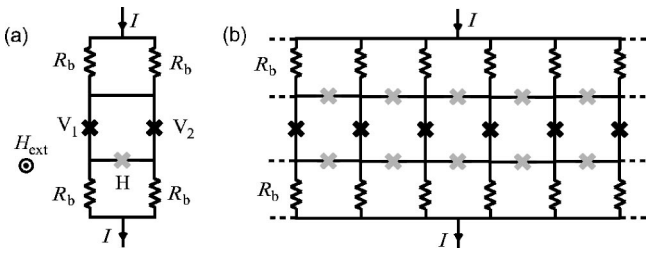

FIG. 1. Sketch of the single-cell system (a) and of the Josephson ladder (b). Josephson junctions are indicated by crosses, superconducting leads by straight lines. The homogeneous bias current I is injected through resistors R_B.

simple model[12] describing the phase dynamics of the JL is based on the RCSJ model and neglects mutual inductances between cells.

The vertical JJ's form an array of rotors (pendulums). These JJ's can be driven by a uniform bias current. Technically, this is achieved by using a single current source which feeds a comb of parallel resistors R_B [see Fig. 1(b)]. If the resistance R_B is large enough, the currents through all vertical branches are identical. If the normalized current γ per vertical JJ is large compared to unity, all vertical JJ's rotate. This is the so-called homogeneous whirling state (HWS). In contrast, if the current is small, all JJ's remain in the static state (SS). In the region $4\alpha/\pi<\gamma<1$, the ladder may have some vertical JJ's in the whirling state, while the remaining JJ's are in the static state. In the standard terminology, this localized state is called rotobreather state (RB). Because of the JL geometry, localized voltage states always have to conform to Kirchhoff's voltage law. Hence a single vertical rotating JJ has to be accompanied by one or more horizontal JJ's in the whirling state. A large variety of different RB states is possible, as it has been observed in experiment.[13,8]

The SS of the ladder is influenced by an externally applied magnetic flux $\Phi_{\rm ext}=B_{\rm ext}A$ (due to a magnetic field $B_{\rm ext}$ threading the cell area A). The magnetic field leads to a screening (Meissner) current flowing around the JL. The field may penetrate into the ladder, leading to vortices in the screening current distribution. A measurement of the maximum (critical) current γ_c sustaining the SS reveals information on the magnetic field penetration into the ladder. In Ref. 14, the existence region of the SS of a Josephson ladder was investigated and compared to theoretical predictions..[15] Deviations were found for close to half-integer frustration and attributed to the presence of meta-stable states. In this paper, we present similar measurements of γ_c vs magnetic field and will argue that the deviations are related to the creation of DB's.

When the ladder is in the HWS, all vertical JJ phases rotate at an identical average frequency Ω, while the horizontal JJ's do not rotate. This is accompanied by a uniform voltage drop across the vertical JJ's. Superimposed phase oscillations are strongly enhanced if the rotation frequency Ω matches one eigenfrequency of the cavity formed by the finite ensemble of cells. The enhanced oscillations lead also to an enhanced damping. A suitable experiment is to measure the differential resistance (which is inversely proportional to the damping) of the JL. It is defined as the ratio of voltage change induced by current variation. The matching frequencies (voltage positions) are characterized by steps in the current vs voltage characteristics. Such resonances of the HWS with cavity modes have been studied by Caputo *et al.*[16] A similar behavior was observed when frequency components of a localized RB state coincide with one of the cavity eigenfrequencies.[9,10] We will show experiments where the HWS resonances are found to enforce the creation of symmetry-broken RB states.

We performed the first group of experiments on a single cell, having the central hole area $A=4\times4\ \mu\text{m}^2$, with three small underdamped Nb/Al-AlO_x/Nb JJ's,[17] Fig. 1(a). The vertical JJ's have an area $A_v=6\times6\ \mu\text{m}^2$, while the horizontal JJ has an area $A_h=3\times4\ \mu\text{m}^2$. The anisotropy of the system is then $\eta=A_h/A_v=0.33$. At 4.2 K the parameter of self-inductance evaluated by a measurement of a dc SQUID (superconducting quantum interference device) of the same geometry, is $\beta_L=2\pi LI_{cv}/\Phi_0=0.98$. Measurements were done in a temperature range between 4.2 K and 6.3 K. At each temperature position the damping $\alpha=\pi\gamma_r/4$ and the critical current density j_c are evaluated from the current-voltage characteristic of the HWS. At $T=4.2$ K, $\alpha\simeq0.03$, and $j_c=126$ A/cm^2. The bias current I is introduced via two parallel external resistors, $R_B=1.5\ \text{k}\Omega$, see Fig. 1, so that the bias currents on the two vertical branches are equal. For convenience, the experimental data are shown in the normalized units of the bias current $\gamma=I/I_{cv}$ and frustration $f=\Phi_{\rm ext}/\Phi_0$, where Φ_0 is the flux quantum.

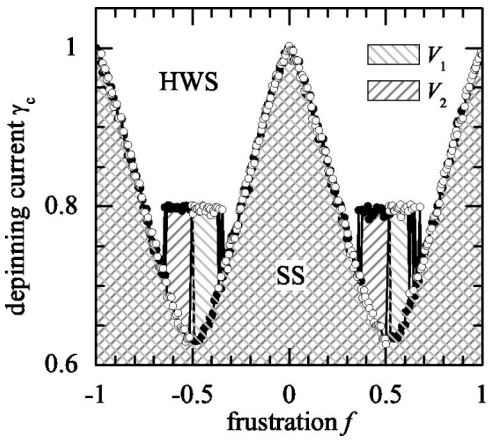

FIG. 2. Dependence of the depinning currents γ_c^1 and γ_c^2 on the external frustration, shown, respectively, by full and open circles. The hatched patterns show the regions where junctions V_1 and V_2 are in the SS.

We ramped up the bias current γ and registered a transition of the system to a resistive state by detecting a nonzero voltage at either junction V_1 (this critical value of γ we call γ_c^1) or junction V_2 (we call it γ_c^2). The measured dependence of γ_c^1 and γ_c^2 on the external magnetic field is, as expected,[11] periodic, see Fig. 2. Around $f=\pm0.5$, the behavior of the two vertical JJ's is found to differ and spontaneous formation of broken-symmetry states[10] is observed. In Fig. 2 the experimental data at $T\simeq6$ K are shown. At this temperature, the parameters of the cell are $\alpha\simeq0.09$, $\beta_L\simeq0.7$, $j_c\simeq95$ A/cm^2, $\omega_p/2\pi=55$ GHz. In the range of frustration $-0.7\lesssim f\lesssim-0.5$ and $0.3\lesssim f\lesssim0.5$, where large clockwise mesh currents are induced, the junction V_1 remains in the SS while the junction V_2 switches to the resistive state. The junction V_1 switches to the resistive state at a higher current about $\gamma\simeq0.8$ that limits the existence of this broken-symmetry breather state.[18,10] As expected, the maximum value of the bias current that allows for the existence of the breather state does not depend on the frustration.[10] In the range $-0.5\lesssim f\lesssim-0.3$ and $0.5\lesssim f\lesssim0.7$, large counter-clockwise mesh currents are induced. The junction V_1 switches first and the second possible breather state is spon-

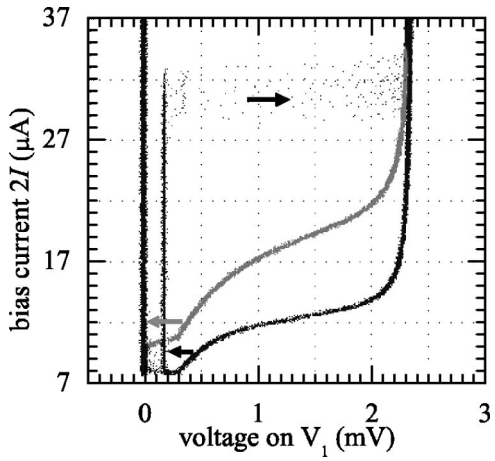

FIG. 3. Dynamic switching from the resonance of the HWS (black dots, with a resonant step at about 0.2 mV) to the broken symmetry state (gray points); $f=-0.41$.

taneously induced. The range of frustration, where the magnetic field induced breather states are observed, broadens with temperature.

At temperatures higher than 4.2 K, the HWS current-voltage characteristic in presence of external frustration showed the well-known resonance due to the interaction with the electromagnetic oscillatory modes of the cell.[19,16,20] At $T\simeq 6$ K, for some values of frustration about 0.5, the interaction of the HWS with the oscillatory modes of the cell led the system to switch from the top of the resonance towards a RB state, see Fig. 3.

The second group of experiments has been performed with various open-ended JL's. Ladder 1 consisted of 20 cells, with parameters $\eta=0.5$, $\beta_L\approx 1.2$, and $\alpha\approx 0.03$. Ladder 2 consisted of 10 cells, with $\eta=0.42$, $\beta_L\approx 0.36$, and $\alpha\approx 0.03$. Ladder 3 has $N=10$, $\eta=0.49$, $\beta_L\approx 0.35$, and $\alpha\approx 0.03$. The sample layout is similar to the one presented in Ref. 14. The measurement was performed at a temperature of 4.2 K.

Measurements of the critical current γ_c^i needed to force the vertical JJ *i* to the finite voltage state are presented in Fig. 4. These data were obtained from ladder 1. The pattern of the depinning current γ_c^i is periodic in frustration, with the period corresponding to a magnetic flux of Φ_0 per cell. Around integer values of *f*, the critical currents for left, center, and right positions in the ladder coincide. After the depinning, for $\gamma\geqslant\gamma_c^i$, the HWS is formed. For $f\sim 0.5$, the critical currents γ_c^i differ for voltages measured on different positions in the ladder. At $-0.35\lesssim f\lesssim -0.25$ and $0.65\lesssim f\lesssim 0.7$, the right and central vertical JJ's of the ladder start to rotate at a lower value of γ than the left part of the ladder. For $0.35\lesssim|f|\lesssim 0.65$, the central part depins at the lowest value of the current ($\gamma\approx 0.7$), the right part at an intermediate current ($\gamma\approx 0.8$), and the left part at the highest value of the current ($\gamma\approx 0.85$). For $-0.75\lesssim f\lesssim -0.65$ and $0.25\lesssim f\lesssim 0.35$, the center and left parts depin for a low current and the right part depins at a higher current.

In Fig. 5, we present similar measurements for ladder 2. These data qualitatively resemble those of Fig. 4. However,

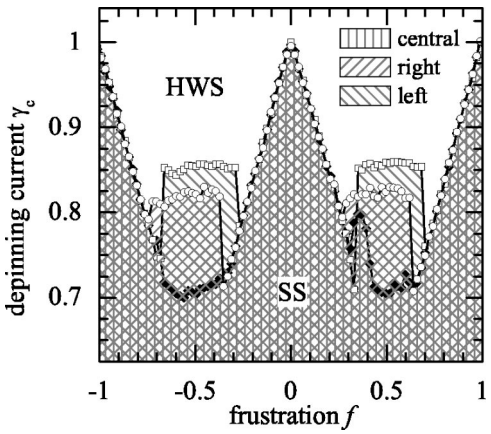

FIG. 4. Dependence of the left (open squares, γ_c^1), central (filled diamonds, γ_c^{11}), and right (open circles, γ_c^{21}) vertical junction depinning currents on the frustration *f*, measured on ladder 1 with $N=20$, $\eta=0.5$, $\beta_L\approx 1.2$.

the minimum depinning currents in the central region around $0.3\lesssim|f|\lesssim 0.7$ are lower, here the central region depins at $\gamma\approx 0.4$. The left and right side of the ladder depin for $\gamma\approx 0.5$.

By definition, a breather state is formed when one part of the vertical JJ's in the ladder rotates while the rest of it remains in the SS. Hence in the described frustration regions around $f\sim 0.5$, breathers are found. They form solely due to an external magnetic field. Because of the limited number of voltage probes in our long ladder, we were not able to exactly identify the precise number of rotating JJ's in the breather states which were formed, but could clearly distinguish them from the HWS.

Our observations can be qualitatively explained in the following way. When the HWS has formed for large γ and finite frustration *f*, magnetic flux penetrates into the system via the boundary cells. When γ is reduced to zero, the ladder settles in the SS, which may be a metastable state or the system ground state. Above some critical value of the frustration f_c, this state consists of a nonzero amount of

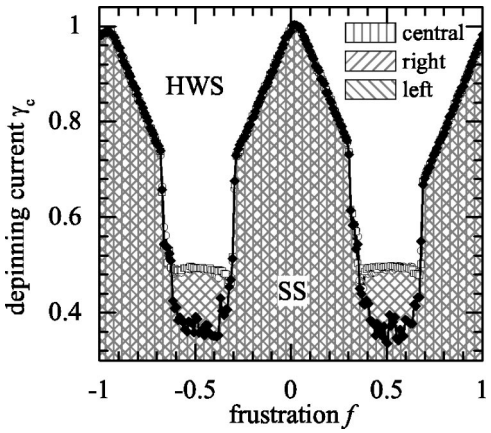

FIG. 5. Frustration dependence of the left (squares, γ_c^1), central (diamonds, γ_c^6), and right (circles, $\gamma_c^1 1$) vertical junction depinning currents for ladder 2 with $N=10$, $\eta=0.42$, and $\beta_L\approx 0.36$.

vortices.[15] The critical field permitting a stable static vortex inside a ladder is estimated[21] as

$$f_c \approx \frac{1}{\pi} \arcsin\left(\frac{1-\eta^2}{1+\eta^2}\right). \quad (2)$$

Using the parameters from Fig. 5, we obtain $f_c = 0.26$, which fits the region of suppressed depinning currents reasonably. For small bias currents γ, the vortices are pinned due to the lattice discreteness. The depinning current can be estimated from the effective discreteness $\beta_{L,\mathrm{eff}} = \beta_L + 2/\eta$ in the static case[14] and the corresponding depinning current γ_{dep} in the discrete sine-Gordon chain, as suggested by Trias *et al.*[21] For the parameters of Fig. 5, we obtain $\gamma_{\mathrm{dep}} \approx 0.4$ which nicely fits the experimental γ_c.

When the vortices start to move, they may ultimately bump into the ladder boundary. This will eventually force the boundary JJ to the whirling state, with the rest of the ladder remaining in the static state. The low value of η is crucial for the observed behavior. Preliminary numerical simulations have shown this kind of behavior for typical experimental parameters.[22]

We note here that a qualitatively similar observation was presented in Ref. 23, where a mechanical model of the discrete damped and driven sine-Gordon chain was studied. A dense chain of vortices hitting the boundary resulted in the rotation of the boundary part of the chain, while the remaining part of chain was static. After some time, the rotation was reversed and the opposite part of the system started rotating. However, the described phenomenon does not represent a *persisting* localized state. Due to the topological difference of the discrete sine-Gordon model and the system studied here, in our case the localized rotating state persists with time, representing a discrete breather in the strict sense.

For longer systems, it is also expectable and observed that moving vortices may be expelled via one of the horizontal JJ's *before* reaching the boundary. When a vortex passes ''through'' a horizontal junction, this phase may be left rotating, again leading to the formation of a RB. A series of DB's may be left behind a moving vortex. This has been observed also in the simulations presented in Fig. 6 of Ref. 21. We conclude that the depinning transitions for JL's with low anisotropy η can lead to the formation of *localized whirling RB states*.

We also observed the creation of a RB state from a *resonant* HWS in JL's. These experiments were performed with ladder 3 (parameters given above). In the presence of the external magnetic field, we observe resonant steps on the current-voltage characteristics of the ladder, as shown in Fig. 6. They occur when the vertical JJ rotation frequency Ω matches one of the cavity eigenfrequencies, as discussed in Ref. 16. When the homogeneous current is increased at a resonance, the amplitude of the cavity oscillations increases. If the driving current becomes too large, the resonant state cannot be maintained anymore and the nonresonant HWS (now with a larger rotation frequency) is retained. This hysteretic process is usually repeatable for an arbitrary number of times. However, in some rare but reproducible cases, we

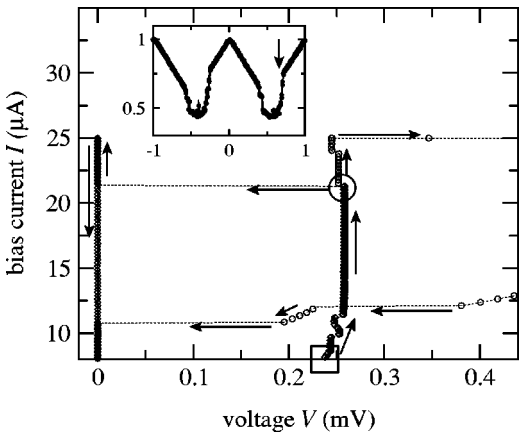

FIG. 6. Current-voltage curve of ladder 3 with $N = 10$, $\eta = 0.49$, and $\beta_L \sim 0.35$, indicating the creation of a breather state from a whirling mode resonance for a frustration $f = 0.66$. The current was swept from $I = 8.4$ μA to $I = 25$ μA and back. Both the central (circles) and the right boundary (diamonds) voltages are plotted. Arrows indicate directions of the voltage switching and the path which is taken during the current sweep. The square indicates the initially prepared resonant HWS ($I = 8.4$ μA). The circle indicates the position at which the symmetry-broken state is formed ($I = 21.4$ μA). The inset shows the dependence of the center junction depinning current on frustration, the arrow marks the frustration at which the current-voltage curve was taken.

observed a transition from such a resonant, spatially homogeneous state towards a localized RB state. The localized state RB can be identified as before by a zero voltage drop across some vertical JJ's in parallel with a finite voltage drop across another group of vertical JJ's. In Fig. 6, the voltage switching, and hence the RB formation happens in the region emphasized by the circle, around $I = 21.4$ μA. During further increase of the current the RB voltage stays constant, apart from some tiny jumps. We thus observe here that a *resonant* RB state is formed from the resonant HWS. Ultimately, the RB voltage switches to a high value (at $I \approx 25$ μA). Here the breather state is still present, but is nonresonant. The tiny voltage jumps along the RB resonance may indicate either transitions between different excited modes or a change in the RB size, which could not be detected in this experiment due to the limited number of voltage probes. The described transition occurs for a very narrow range of magnetic field.

In summary, we reported here on the spontaneous creation of discrete breather states in single Josephson plaquettes and Josephson ladders. The excitation of breather states is observed during the transition from the static to the whirling state of the array, resulting from a ramp of an externally applied homogeneous bias current. In another regime, the breather states are created from the resonant uniformly whirling state of the array. The spontaneous creation appears in the presence of an external magnetic field close to half-integer frustration, which leads to large screening currents. The observed behavior may be related to the appearance of symmetry-broken states in two-dimensional Josephson arrays.[24] An analysis of the described phenomena could provide more insight in the physical relevance of intrinsic localized voltage states in Josephson coupled systems.

[1] S. Aubry, Physica D **103**, 201 (1997).
[2] S. Flach and C.R. Willis, Phys. Rep. **295**, 181 (1998).
[3] B.I. Swanson, J.A. Brozik, S.P. Love, G.F. Strouse, A.P. Shreve, A.R. Bishop, W.-Z. Wang, and M.I. Salkola, Phys. Rev. Lett. **82**, 3288 (1999).
[4] U.T. Schwarz, L.Q. English, and A.J. Sievers, Phys. Rev. Lett. **83**, 223 (1999).
[5] E. Trías, J.J. Mazo, and T.P. Orlando, Phys. Rev. Lett. **84**, 741 (2000).
[6] P. Binder, D. Abraimov, A.V. Ustinov, S. Flach, and Y. Zolotaryuk, Phys. Rev. Lett. **84**, 745 (2000).
[7] J.J. Mazo, E. Trías, and T.P. Orlando, Phys. Rev. B **59**, 13 604 (1999).
[8] P. Binder and A.V. Ustinov, Phys. Rev. E **66**, 016603 (2002).
[9] M. Schuster, P. Binder, and A.V. Ustinov, Phys. Rev. E **65**, 016606 (2001).
[10] F. Pignatelli and A.V. Ustinov, Phys. Rev. E **67**, 036607 (2003).
[11] A. Barone and G. Paternó, *Physics and Applications of the Josephson Effect* (Wiley, New York, 1982).
[12] G. Grimaldi, G. Filatrella, S. Pace, and U. Gambardella, Phys. Lett. A **223**, 463 (1996).
[13] P. Binder, D. Abraimov, and A.V. Ustinov, Phys. Rev. E **62**, 2858 (2000).
[14] P. Binder, P. Caputo, M.V. Fistul, A.V. Ustinov, and G. Filatrella, Phys. Rev. B **62**, 8679 (2000).
[15] M. Barahona, S.H. Strogatz, and T.P. Orlando, Phys. Rev. B **57**, 1181 (1998).
[16] P. Caputo, M.V. Fistul, A.V. Ustinov, B.A. Malomed, and S. Flach, Phys. Rev. B **59**, 14 050 (1999).
[17] HYPRES Inc., Elmsford, NY 10523.
[18] M.V. Fistul, S. Flach, and A. Benabdallah, Phys. Rev. E **65**, 046616 (2002).
[19] M. Barahona, E. Trias, T.P. Orlando, A.E. Duwel, H.S.J. van der Zant, S. Watanabe, and S.H. Strogatz, Phys. Rev. B **55**, 11 989 (1997).
[20] P. Caputo, M.V. Fistul, and A.V. Ustinov, Phys. Rev. B **63**, 214510 (2001).
[21] E. Trías, J.J. Mazo, and T.P. Orlando, Phys. Rev. B **65**, 054517 (2002).
[22] M. Schuster, PhD thesis, Universität Erlangen-Nürnberg, 2004.
[23] M. Cirillo, R.D. Parmentier, and B. Savo, Physica D **3**, 565 (1981).
[24] D. Abraimov, P. Caputo, G. Filatrella, M.V. Fistul, G.Y. Logvenov, and A.V. Ustinov, Phys. Rev. Lett. **83**, 5354 (1999).